RSC Advances

ROYAL SOCIETY OF CHEMISTRY

www.rsc.org/advances

RSC Advances

RSCPublishing

COMMUNICATION

The Hydrogenation of aromatic-naphthalene with Ni_2P/CNTs

Minzhi Ruan,[a] Jun Guan,[a] Demin He,[a] Tao Meng,[c] Qiumin Zhang *[a, b]

Cite this: DOI: 10.1039/x0xx00000x

Received ooth January 2015,
Accepted ooth January 2015

DOI: 10.1039/x0xx00000x

www.rsc.org/

Ni_2P/CNTs is synthesized by impregnation method. The XPS reveals CNTs could affect the electronic properties of bulk Ni_2P. The catalyst shows superior activity for HYD of naphthalene with a conversion of 99%, and reflects superior tolerance towards potential catalyst poisons, which is higher than Ni/CNTs of 89%.

Due to the increasing low quality petroleum feedstocks and increasingly stringent environmental regulations, it is paramount important to develop new environmentally friendly catalyst for hydrotreating. The Hydrogenation (HYD) and Hydrodesulfurization (HDS) reactions, which transfer polycyclic aromatic hydrocarbons with sulfur into high RON oil and underpins many clean-energy technologies. Although the Pt or Pd has been used as the hydrotreating catalyst, they have bad performance when contact with sulfur.[1] Furthermore Pt and Pd are luxurious and relatively infrequent in the Earth's shell limiting the utility of them in energy systems deployed at global scale. More recently, nanoparticulate films of Ni_2P comprised of inexpensive to show high HDS activity. As the nickel phosphorus catalyst first introduced by Oyama, it has aroused lots of interests all around the world, as it was used in the energy application with a high performance of HDS and Hydrodenitrogenation (HDN) activity or even have an outstanding performance in the fuel cell. It indicated the sequence of HYD activity over transition metal phosphides is as follows: Fe_2P<CoP<MoP<WP<Ni_2P, the Ni_2P catalyst is found to be the most active.[2-4] Among such classes of catalysts, various carbon nanostructures, including carbon, carbon nanotubes, and grapheme and so on, have been used for the catalyst carriers which have an excellent performance.[5-6] However, carbon nanotubes (CNTs) with unique properties have experienced limited used as support material for Ni_2P, and the potential industrial application value of Ni_2P/CNTs in aromatic HYD has not been sufficiently explored. Herein, we have thus applied Ni_2P catalysts supported on carbon nanotubes to examine the effect of HYD. The CNTs has huge specific area which has been reported as it has better hydrogen storage function and strictly mesoporous nature, differing largely from the classical activated carbon support.[7-13] It was functionalized with mixed acid which led to the unique CNT properties, and the Ni_2P/CNTs particles were synthesized using impregnation method.[14]

X-ray diffraction patterns of reduced Ni_2P/CNTs and Ni_2P samples are presented in Fig.1a. The Ni_2P loadings were varied from 5 to 40 wt%，and the Ni/P mole ratio were varied from 0.5 to 2.0. With the increase of Ni_2P loading and Ni/P mole ratio, the sharp and symmetric peaks evidently indicate that the samples were well crystallized. The patterns all display a broad feature at 20~30° and 48.8°due to the carbon tubes support. For all catalyst, the peaks at 2θ=40.6°, 44.5°, 47.1°, 54.1°, 54.8° (PDF:74-1385) can be ascribed to Ni_2P, and no additional phase of Ni and P is observed, indicating that the active phase formed is mainly Ni_2P for all samples. The coexistence of Ni_2P and CNTs in the sample (Fig.1b) was substantiated by Energy dispersive spectroscopy (EDS) in Fig.1c.

The IR spectrum of functionalized CNTs and Ni_2P/CNTs are given in Fig.1d. The bands appearing at 1000 cm^{-1} can be assigned to the Ni_2P,and the bands appearing at 1635 and 3450 cm^{-1} can be assigned to the C=O and O-H stretching vibration bands, which confirmed the presence of functional groups in the acid-treated CNTs, which could help adsorb active metal on the surface.[15]

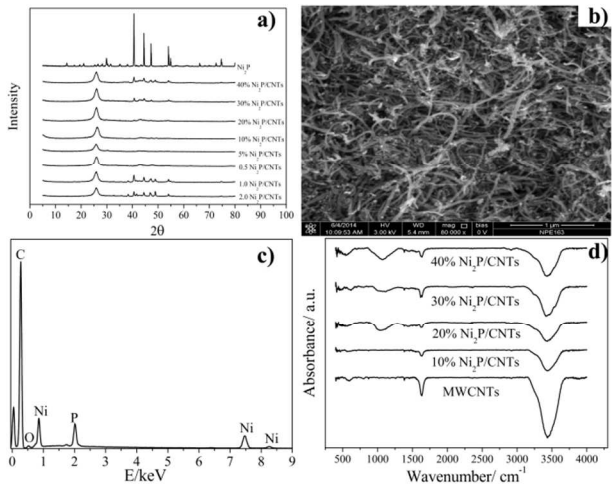

Fig.1 (a)XRD patterns of catalyst samples with different wt% of Ni_2P (Ni/P=1.25, atomic) and Ni/P proportion (30 wt% Ni_2P); (b) SEM image of the 30 wt% Ni_2P/CNTs; (c) EDS of 30 wt% Ni_2P/CNTs; (d) FTIR of catalyst samples.

Table 1. BET results and pore structure parameter of Ni_2P/CNTs catalysts.

Samples	Surface area (m^2/g) [a]	Pore volume (cm^3/g) [a]	dXRD (nm) [b]	dTEM (nm) [c]
10wt%	171	0.33	13.6	6.7
20wt%	151	0.31	14.6	11.0
30wt%	143	0.26	21.9	13.1
40wt%	94	0.23	28.0	20.0

[a] Evaluated from N_2 adsorption-desorption isotherms

[b] Calculated by Scherrer equation from the XRD

[c] Measured by TEM

Table 1 shows the physical properties for the Ni_2P/CNTs, including the Ni_2P loading contents, averaged Ni_2P size and BET surface area. The results showed that BET surface area of the catalysts declined with the increase in the amount of Ni_2P loading. It indicated that the Ni_2P particles occupied the surface hole of the CNTs. TEM observations indicate that the size and the morphology of the Ni_2P/CNTs composites are differ from those of CNTs. Most of Ni_2P particles display outside the CNTs, the loading content could affect the Ni particle size and its distribution.[15] In addition, as the histograms were given in Fig.2, in which the mean size of increase from 6.7 nm to 20.0 nm with the increasing of loading content. In the following section, it was found smaller Ni_2P particle size with a higher dispersion which contributes to inhibit the agglomeration of Ni_2P particles should be favour to the hydrogenation reaction.

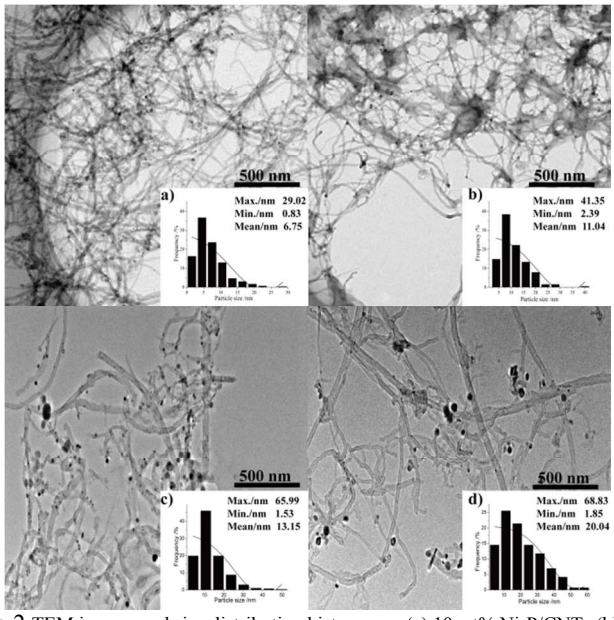

Fig.2 TEM images and size distribution histograms: (a) 10 wt% Ni_2P/CNTs (b) 20 wt% Ni_2P/CNTs. (c) 30 wt% Ni_2P/CNTs. (d) 40 wt% Ni_2P/CNTs.

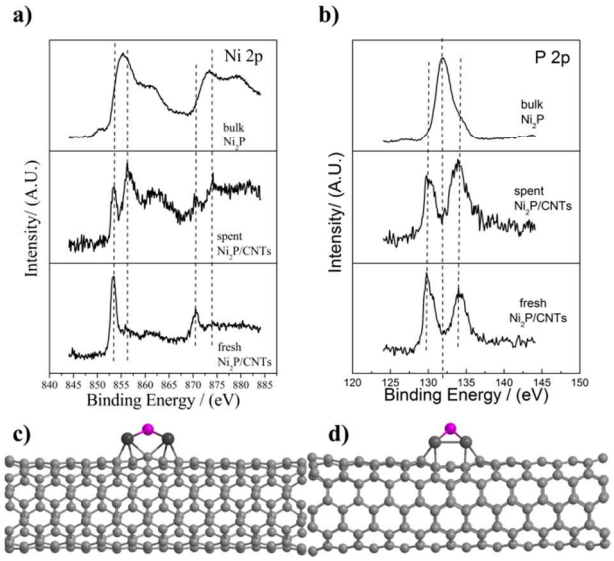

Fig.3 XPS spectra for Ni_2P, spent Ni_2P/CNTs and fresh Ni_2P/CNTs: (a) Ni 2p core level spectra and (b) P 2p core level spectra. The two stable binding sites for Ni_2P on CNTs: (c) atop-atop site and (d) bridge-bridge site.

The XPS Ni 2p and P 2p spectra of 30 wt% Ni_2P/CNTs catalysts are presented in Fig.3a-b. For samples (1)-(3), Ni 2p core level spectrum includes two contributions (Fig.3a-b), which correspond to Ni 2p 3/2 and Ni 2p 1/2, respectively. The former one, is assigned to Ni δ+ in Ni 2p phase and centered at 853.31 eV, and the later one at 857.9 eV is oxidized Ni. With regards to P 2p 3/2 binding energy, the peaks of P 2p electron binding energy at 129.87 eV and 133.98 eV can be assigned to oxidized and elemental P, respectively.

The peaks in the XPS spectrum for the Ni_2P catalyst have been assigned previously.[16-17] For Ni_2P, the binding energies at 857.9 and 134.8 eV are assigned to Ni2+ and P5+ species. The XPS spectrum for 30 wt% Ni_2P/CNTs catalyst commonly mirrors that for the Ni_2P catalyst. The fresh Ni_2P/CNTs sample

displays two distinct peaks, whose positions correspond to the Ni-P and Ni-Ni distances in bulk Ni_2P. The P (2p) region shows one significant difference: the XPS spectrum of Ni_2P catalyst has a very intense peak at 132.04 eV but there are two peaks on the XPS of Ni_2P/CNTs that is consistent with the binding energy for phosphorus in CNTs. Some of the phosphorus impregnated onto the CNTS apparently reacts with the support to form Ni-P-CNTs. The spectrum of the fresh Ni_2P/CNTs differs from Ni_2P sample, indicating that Ni+ peak shifted from 855.4 to 853.31 eV (Fig.3a), and the binding energy assigned to P5+ species shifted from 131.96 to 129.87 eV (Fig.3b). The shift of binding energies of surface Ni+ and P5+ species suggests the existence of an electronic effect caused by the surface –OH or –COOH or CNTs species, which may result in the electron enrichment on the surface Ni and P species. As it is revealed in Fig.3c-d, the Ni atom placed on an atop site instead of at a hole site, there are two stable binding sites for a Ni_2 dimer on carbon nanotube wall: atop-atop site and bridge-bridge site. The Ni_2 dimer when placed on nanotube wall has a tendency to separate in a reaction mediated by the underlying carbon atoms. Thus, the number of Ni_2 configurations on a tube vary with the curvature and Ni_2 exhibits a larger range of Ni-Ni bond lengths (2.34-2.78Å).[18] Significant shift in binding energy peaks assigned to the spent phosphorus species in Ni_2P/CNTs was detected, illustrating that the addition of CNTs could affect the electronic properties of bulk Ni_2P.

Table 2. Catalytic hydrogenation of naphthalene and 1-methyl naphthalene [a]

Samples	Raw materials	Products	Selectivity[%]
30 wt% Ni_2P/CNTs	Naphthalene	Cis-decalin	14
		Trans-decalin	69
		Tetralin	17
30 wt% Ni_2P/CNTs	1-Methyl naphthalene	1-Methyl tetralin	17
		5-Methyl tetralin	36
		1-Methyl decalin	47
20 wt% Ni/CNTs	Naphthalene	Cis-decalin	0
		Trans-decalin	28
		Tetralin	61

[a] Reaction conditions: reactions were carried out with naphthalene or 1-Methyl naphthalene (5 wt% in decane), at 613K, 4.0 Mpa, vapour-liquid ratio=600, LHSV=4.0 h^{-1}. The Ni loading of 20 wt% Ni/CNTs is equal to the Ni loading of 30 wt% Ni_2P/CNTs. Reactions were carried out in a continuous-flow micro reactor.

Table 3. Hydrotreating performance of Ni_2P/CNTs catalysts. [a]

Entry	Ni_2P (wt%)	Ni/P(atomic)	LHSV(h^{-1})	Convention [%]
1	40	1.25	4	91
2	30	1.25	4	>99
3	20	1.25	4	65
4	10	1.25	4	30

[a] Reaction conditions: reactions were carried out with naphthalene (5 wt%), at 613K, 4.0 Mpa.

The hydrotreating reaction results for the Ni_2P/CNTs in the HYD of naphthalene and 1-methyl naphthalene are summarized in Table 2 and Table 3. Mass balance is 100±5% for each reaction type. The reaction of naphthalene on the 30 wt% Ni_2P/CNTs(Ni/P=1.25, mol) occurs with a very high and stable conversion of 99%, which is much higher than other samples or that of the Ni_2P/SiO_2 catalyst, the NiP/C catalyst.[8,20] This may be attributed to the 30 wt% Ni_2P/CNTs has higher BET surface area which could provide more Ni_2P active sites on the surface of CNTs(Table 1), furthermore, the Ni_2P particles of 30wt% samples with small size were well dispersed on the CNTs(Fig 2). There are three major products formed from naphthalene on these catalysts: cis-decalin, trans-decalin and tetralin compared with the Ni_2P/SiO_2 catalysts, the Ni_2P/CNTs gave a higher trans-Decalin selectivity of 69% and the proportion of cis-Decalin and trans-decalin is nearly to 1:4, indicating that it favours the hydrogenation pathway. In comparison with naphthalene, tetralin，the final products of HYD of 1-methyl naphthalene is fewer than 50%, this is due to the steric hindrance effect caused by methyl. The Ni/CNTs catalyst exhibits less activity with a conversion of 84%. Obviously, the existence of P contributes to the HYD; the joint action of Ni-P-CNTs effect could explain by XPS results. Liu et al. also confirmed the P sites of the phosphide of Ni_2P play a complex and significant role. First, the Ni-P bonds produce a weak ligand effect that allows a reasonably high activity for HYD. Second, the Ni active sites on the surface declines owing to an ensemble effect of P, which prevents the reaction system from the deactivation. Third, the P sites are spectators and provide moderate bonding and the H adatoms essential for HYD.[21]

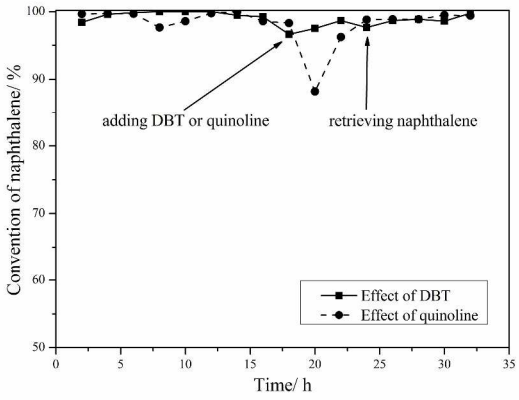

Fig.4 Effect of adding DBT or quinolone to HYD. The content of HDS and HDN intermediates of DBT and quinoline was 1.0 wt% in 5.0 wt% naphthalene reactant.

We next investigated the durability and the resistance to sulfur and nitrogen solution of the catalysts. As it clearly revealed in Fig.4, after contacted with sulfur and nitrogen solution, the initial HYD convention dropped from 99% to 85%, while when the solution were switched to naphthalene, the catalyst can retrieve to the former level, it reflects superior tolerance towards potential catalyst poisons, such as DBT and quinoline.

In summary, a novel Ni_2P/CNTs catalyst was developed for HYD. The catalyst exhibit excellent activity and stability, and was successfully used for HDS or HDN, showing superior performance to a Pt-Pd catalyst. As aromatic compounds are important component of fuels, the work is a significant step towards the development of more active and practical catalysts for upgrading of Coal-tar and Bio-oil.

Experimental Section

Multi-carbon nanotubes were purchased from CAS. (Chengdu, China). Concentrated nitric acid (70%, Aladdin) was used to functionalize CNTs at 60℃ for 6h. Nickel phosphate compounds loading with CNTs were prepared by the following

route: Nickel nitrate (60mg, 99%, Aladdin) and ammonium hydrogen phosphate (20mg, 99%, Aladdin) were dissolved in deionized water. Functionalized CNTs (100mg) were then mixed into the solution. Ultrasonication was carried out for 6h and followed by impregnation at room temperature. The sample was then collected and calcined in the N_2 at 793K. Reduction was conducted in 95% H_2 mixed with 5% He in a total flow of 100 mL/min at 793K. Subsequently, the calcined sample was pelletized and sieved for HYD reaction.

Acknowledgements

The authors thank for the financial supports of Major Project of the National Energy Administration (NY20130302513-1).

Notes and references

[a] School of Chemical Engineering, Dalian University of Technology (DUT), No.2 Linggong Road, Dalian 116024, P. R. China.
E-mail: zhangqm@dlut.edu.cn.
[b] State Key Laboratory of Fine Chemicals, Dalian University Of Technology(DUT).
[c] Beijing Guodian Longyuan Environmental Engineering Co., LTD, Building No.1, Yard No.16, Xisihuan Mid Road, Haidian District, Beijing 100039, PR China
*Corresponding author. Tel.: +86 0411 84986150; Fax: +86 0411 84986150
E-mail: zhangqm@dlut.edu.cn
†Electronic Supplementary Information (ESI) available: [details of any supplementary information available should be included here]. See DOI: 10.1039/c000000x/

1 H. Song, J. Wang, Z. Wang, H. Song, F. Li, Z. Jin, Journal of Catalysis 2014, 311, 257.
2 S. T. Oyama, Journal of Catalysis 2003, 216, 343.
3 A. Infantes-Molina, J. A. Cecilia, B. Pawelec, J. L. G. Fierro, E. Rodríguez-Castellón, A. Jiménez-López, Applied Catalysis A: General 2010, 390, 253.
4 J. Chang, L. Feng, C. Liu, W. Xing, X. Hu, Angewandte Chemie International Edition 2014, 53, 122.
5 Y. Shu, S. T. Oyama, Carbon 2005, 43, 1517.
6 Y. Lu, J. Tu, Q. Xiong, Y. Qiao, J. Zhang, C. Gu, X. Wang, S. X. Mao, Chemistry - A European Journal 2012, 18, 6031.
7 Y. Lu, X. Wang, Y. Mai, J. Xiang, H. Zhang, L. Li, C. Gu, J. Tu, S. X. Mao, The Journal of Physical Chemistry C 2012, 116, 22217.
8 A. C. Dillon, K. M. Jones, T. A. Bekkedahl, C. H. Kiang, D. S. Bethune and M. J. Heben, Nature, 1997, 386, 377-379.S. T. Oyama, X. Wang, Y. K. Lee, W. J. Chun, Journal of Catalysis, 2004, 221, 263.
9 E. G. Rodrigues, S. A. C. Carabineiro, J. J. Delgado, X. Chen, M. F. R. Pereira and J. J. M. Órfão, Journal of Catalysis, 2012, 285, 83-91.
10 F. Zhu, G. Ma, Z. Bai, R. Hang, B. Tang, Z. Zhang and X. Wang, Journal of Power Sources, 2013, 242, 610-620.
11 D. Z. Mezalira and M. Bron, Journal of Power Sources, 2013, 231, 113-121.
12 V. Lordi, N. Yao and J. Wei, Chemistry of Materials, 2001, 13, 733-737.
13 S. M. Bachilo, L. Balzano, J. E. Herrera, F. Pompeo, D. E. Resasco and R. B. Weisman, Journal of the American Chemical Society, 2003, 125, 11186-11187.
14 M. Moula, S. Suzuki, W. Chun, S. Otani, S. T. Oyama, K. Asakura, Others, Surface and interface analysis 2006, 38, 1611.
15 Zhou M, Zhu H, Niu L, et al. Catalysis letters, 2014, 144(2): 235-241.
16 D. Kanama, Surface Science Spectra 2001, 8, 220.
17 P. Liu, J. A. Rodriguez, Y. Takahashi, K. Nakamura, Journal of Catalysis 2009, 262, 294.
18 M. Menon, A. N. Andriotis, G. E. Froudakis, Chemical Physics Letters 2000, 320, 425.
19 D. S. Misra, A. Misra, P. K. Tyagi, M. K. Singh, Diamond and Related Materials 2006, 15, 385.
20 S. Yang, R. Prins, Chemical Communications 2005, 4178.
21 Liu P, Rodriguez J A, Asakura T, et al. The Journal of Physical Chemistry B, 2005, 109(10): 4575-4583.

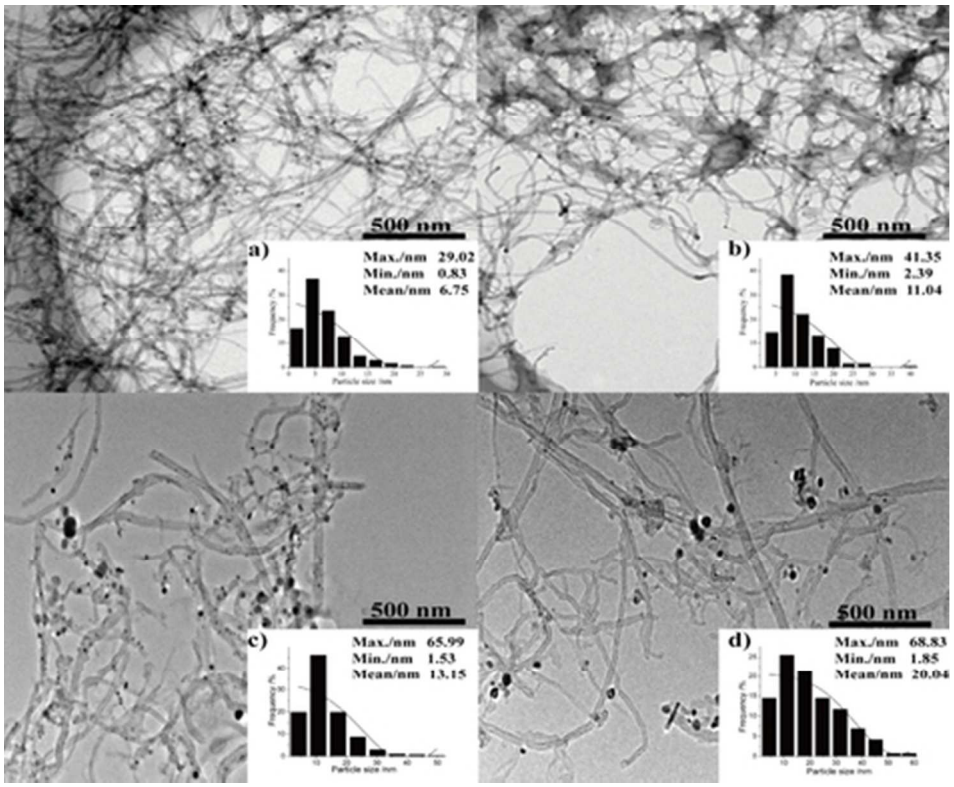

39x32mm (300 x 300 DPI)